

Thermal Characteristics of Brillouin Microsphere Lasers

Kaijun Che¹, Deyu Tang, Changyan Ren, Huiying Xu², Lujian Chen, Chaoyuan Jin, and Zhiping Cai¹

Abstract—In this paper, we investigate the thermal characteristics of Brillouin microsphere lasers. A mathematical model for Brillouin lasing in a waveguide coupled microcavity is constructed based on the coupled mode theory, the analytic correlation between lasing and thermal power is given. To track the thermal responses of Brillouin microlasers, we introduce two kinds of thermal perturbations on the packaged silica microspheres by either tuning the wavelength of pump wave or varying the surrounding temperature. It is shown that the output power of Brillouin lasers is sensitive to and linearly varied with the thermal change of the mode area and surroundings. The optical bistabilities induced by the resonances transitions of the pump wave and Brillouin lasing, and a single mode lasing with up to 41.7-dB side mode suppression ratio are demonstrated. Our results demonstrate that Brillouin microlasers with stable performances hold potential for sensor applications since thermal or optical perturbations on microcavity can be simply tracked by the variation of output power.

Index Terms—Brillouin microlaser, thermal characteristics, microsphere cavity.

I. INTRODUCTION

BRILLOUIN lasing or stimulated Brillouin scattering (SBS) is a coherent nonlinear phenomenon originated from the inelastic scattering of material lattice, where a pump signal wave and the scattered Stokes wave interferes with each other and the mechanical oscillation induced by the electrostriction effect is formed as an acoustic wave at certain frequency [1]–[4]. In the past decades, the SBS has attracted intensive interests for its unique features, such as low threshold and ultra-narrow linewidth [4], and been widely developed and investigated in fiber-based system [3], in on-chip photonic circuits [5]–[7] and in whispering gallery mode (WGM) microcavities [8]–[11]. WGM microcavities with high-Q resonances can greatly enhance the light-matter interaction and have become a promising platform for the achievement of

low threshold SBS [8]–[18]. Up to date, a variety of cavities have already been employed for SBS, such as silica/tellurite microspheres [10]–[14], silica rods/microbottles/bubbles [15]–[17], and silica/fluoridemm-disks [9], [18]–[20]. The SBS can be effectively excited when both pump and scattered Stokes waves are involved into cavity resonances. In addition, some SBS applications, such as microwave synthesizers and filters [21], [22], slow light for light storage [23], [24], and gyroscopes [25], have been recently reported. Among all the above mentioned cavities, silica sphere cavities with dimensions of hundreds micrometers possess unique features of ultra-rich mode resonances and simple fabrication process [26], which enables the thermal latching of pump wave to one of WGM resonances fairly easily and is particularly suited for the SBS realization without repeated sweeping of pump wave.

In this work, thermal characteristics of Brillouin silica microsphere lasers are investigated based on an analytic model and thermal perturbations. In section II, we construct a mathematical model for Brillouin lasing in fiber taper coupled microcavities based on coupled mode theory and obtain an analytic correlation between Brillouin lasing output and thermal power. In section III, two kinds of thermal perturbations, by either tuning the pump wave or varying the surrounding temperature, are proposed for the study of thermal responses of Brillouin lasing. In section IV, we perform the experimental investigations by employing the mechanically packaged silica sphere resonators and verify that the lasing output is sensitive to and linearly varied with the resonant shift that is induced by the thermal perturbation. Some lasing behaviors, such as optical bistabilities due to the resonance transition of pump wave and Brillouin lasing, and up to 41.7dB of side mode suppression ratio (SMSR) are presented. Finally, the conclusions are given in Section V.

II. MATHEMATICAL MODEL OF BRILLOUIN LASING

Fig. 1(a) shows a schematic plot of fiber taper coupled microsphere. In the mathematical model, we define $s_{in}(t)$ and $s_t(t)$ as amplitudes of incident and transmitted waves in the taper while $P_{in} = |s_{in}(t)|^2$ and $P_t = |s_t(t)|^2$ represent the incident and transmitted pump powers. The pump power coupled into cavity P_c is equivalent to $P_{in} - P_t \cdot b_0(t)$ and $b_j(t)$ denote energy amplitudes of the pump wave (regarded as the 0th-order Brillouin lasing) and the j^{th} -order Brillouin lasing as $W_0 = |b_0(t)|^2$ and $W_j = |b_j(t)|^2$ represent their energies stored in the microsphere, respectively. Based on coupled mode theory [27], similar to the theoretical model for

Manuscript received January 10, 2018; revised March 27, 2018 and April 19, 2018; accepted April 20, 2018. Date of publication April 25, 2018; date of current version May 10, 2018. This work was supported in part by the China Scholarship Council under Grant 201606315025 and in part by the National Science Foundation of China under Grant 11674269, Grant 61675172, and Grant 61574138. (Corresponding author: Kaijun Che.)

K. Che, D. Tang, C. Ren, H. Xu, L. Chen, and Z. Cai are with the Department of Electronics Engineering, Xiamen University, Xiamen 361005, China (e-mail: chekaijun@xmu.edu.cn; 544921369@qq.com; 924066252@qq.com; xuhu@xmu.edu.cn; lujianchen@xmu.edu.cn; zpcai@xmu.edu.cn).

C. Jin is with the College of Information Science and Electronic Engineering, Zhejiang University, Hangzhou 310007, China, and also with the Department of Electronic and Electrical Engineering, The University of Sheffield, Sheffield S3 7HQ, U.K. (e-mail: jincy@zju.edu.cn).

Color versions of one or more of the figures in this paper are available online at <http://ieeexplore.ieee.org>.

Digital Object Identifier 10.1109/JQE.2018.2829986

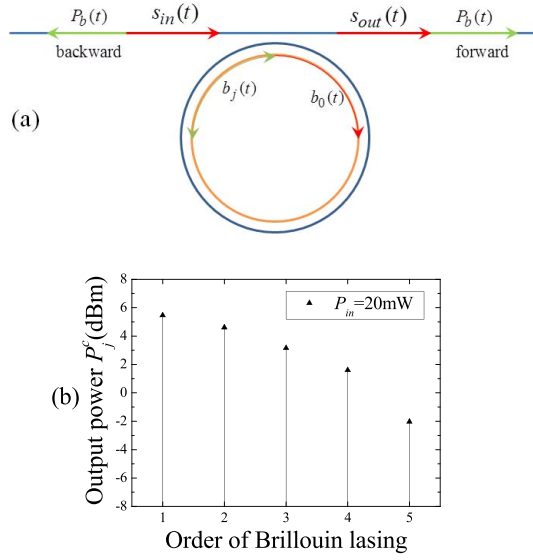


Fig. 1. (a) Schematic plot of a fiber taper coupled microsphere; (b) An example of the output power versus the order of cascaded Brillouin lasing when $P_{in} = 20\text{mW}$.

Raman lasing [28], we can construct the following equations to describe the time evolution of $b_j(t)$

$$\begin{cases} \frac{\partial b_0}{\partial t} = (i\Delta\omega_0 - \kappa_0 - g_1^s W_1)b_0 + \sqrt{2\kappa_0^c} s_{in} \\ \frac{\partial b_j}{\partial t} = (-\kappa_j - g_{j+1}^s W_{j+1} + g_j^s W_{j-1})b_j \\ (j = 1, 2, \dots, N-1) \\ \frac{\partial b_N}{\partial t} = (-\kappa_N + g_N^s W_{N-1})b_N, \end{cases} \quad (1)$$

where $\Delta\omega_0$ is the detuned angular frequency between pump wave and cavity resonance and the detuning between Brillouin lasing and resonance is set as zero since that Brillouin lasing only happens at resonance. $\kappa_j = \kappa_j^i + \kappa_j^c$ is the total loss rate of energy amplitude which comprises of the intrinsic loss rate κ_j^i and the loss rate κ_j^c associated with waveguide coupling. $\kappa_j^c = \kappa_{ej}^2/2\tau_{cj}$ is related to the field coupling coefficient κ_{ej} between guided modes in taper and microsphere, and the round trip time of WGM $\tau_{cj} = 2\pi R n_{eff,j}/c$ [27]. κ_{ej} is directly determined by the field overlap integral and the matching of propagating constants [29], [30], τ_{cj} is related to the WGM effective refractive index $n_{eff,j}$ and the perimeter of cavity $2\pi R$. The $g_j^s = \Gamma g_0 c^2/(2n^2 V_{mj})$ is defined as intra-cavity Brillouin gain coefficient. For the above mentioned variables, c is the light velocity in vacuum, R is the radius of cavity, g_0 is Brillouin gain in bulk silica, n is refractive index, V_{mj} is mode volume of the j^{th} -order Brillouin lasing coupled WGM, Γ stands for the mode overlap.

The steady performances, at which the powers or energies of both pump wave and Brillouin lasing in microsphere are invariable, are considered. Namely, $\partial b_j/\partial t = 0$. The pump power coupled into microsphere P_c is dissipated into power induced by intrinsic loss and the 1st-order Brillouin lasing power:

$$P_c = 2(\kappa_0^i + g_1^s W_1)W_0. \quad (2)$$

In our model, other power loss routes or nonlinear phenomena are ignored when Brillouin lasing dominates in microsphere. Additionally, P_c can also be derived from the total power P_{in} inserted into to taper for pumping [31]:

$$P_c = \frac{4\kappa_0^c(\kappa_0^i + g_1^s W_1)}{(\kappa_0 + g_1^s W_1)^2 + \Delta\omega_0^2} P_{in}, \quad (3)$$

as $s_r(t) = -s_{in}(t) + \sqrt{2\kappa_0^c}b_0(t)$. By comparing Eq.(2) and Eq. (3), we can obtain a relation between W_1 and W_0 :

$$W_0 = \frac{2\kappa_0^c}{(\kappa_0 + g_1^s W_1)^2 + \Delta\omega_0^2} P_{in}. \quad (4)$$

We know that the power of the j^{th} -order Brillouin lasing $P_j^B = P_j^i + P_j^c + P_{j+1}^B$ includes the intrinsic loss power $P_j^i = 2\kappa_j^i W_j$, the power $P_j^c = 2\kappa_j^c W_j$ coupled out by taper and the power $P_{j+1}^B = 2g_{j+1}^s W_{j+1} W_j$ as the pump source for the next order Brillouin lasing. At the same time, P_j^B originates from P_{j-1}^B and $P_j^B = 2g_j^s W_j W_{j-1}$. Thus we can bridge a relation between W_{j+1} and W_{j-1} :

$$W_{j-1} = \frac{g_{j+1}^s W_{j+1} + \kappa_j}{g_j^s}. \quad (5)$$

For the last order (N^{th}) lasing, W_{N+1} is 0, $W_{N-1} = \kappa_N/g_N^s$ can directly be obtained and then $W_{j=N-1-2m}$ can be deduced from W_{N-1} as $m = 1, 2, 3, \dots$ from Eq.(5). If $N-1-2m = 1$, we can obtain W_0 from Eq. (4), or we can obtain W_1 when $N-1-2m = 0$. Based on the obtained W_0 or W_1 , the energies $W_{j=N+2-2m}$ of the other orders Brillouin lasing can be derived from Eq. (5) as well. Finally, the corresponding Brillouin lasing output and the power induced by intrinsic loss can be obtained:

$$P_j^c = 2\kappa_j^c W_j, \quad (6)$$

and

$$P_j^i = 2\kappa_j^i W_j, \quad (7)$$

from the energy stored in cavity, respectively. Fig. 1(b) shows an example of output power for a 5-order cascaded Brillouin lasing, whereas $P_{in} = 20\text{mW}$, $\kappa_j^i = 0.8\pi \times 10^6\text{Hz}$, $\kappa_j^c = 4\kappa_j^i$, $g_j^s = 1.75 \times 10^{14}\text{Hz}^2/\text{mW}$, and $\Delta\omega_0 = \kappa_j^i$. One thing should be noted that odd and even orders Brillouin lasing propagate in the backward and forward directions, respectively, and here backward Rayleigh scatterings and other optical phenomena are ignored.

Finally, we can obtain the total thermal power P_h generated from material absorption:

$$P_h = \sum_{j=0}^N \delta_j P_j^i, \quad (8)$$

δ_j is thermal conversion coefficient of the intrinsic optical losses.

For the single Brillouin lasing ($N = 1$), the output P_1^c and thermal power P_h are derived as:

$$P_1^c = 2\kappa_1^c \sqrt{\frac{2\kappa_0^c P_{in}}{\kappa_1 g_1^s} - \left(\frac{\Delta\omega_0}{g_1^s}\right)^2} - \frac{2\kappa_1^c \kappa_0}{g_1^s}, \quad (9)$$

and

$$P_h = \delta \left[2\kappa_1^i \sqrt{\frac{2\kappa_0^c P_{in}}{\kappa_1 g_1^s} - \left(\frac{\Delta\omega_0}{g_1^s}\right)^2} - \frac{2(\kappa_1^i \kappa_0^c - \kappa_0^i \kappa_1^c)}{g_1^s} \right]. \quad (10)$$

Here δ is defined as the averaged thermal conversion coefficient for intrinsic optical losses of pump wave and Brillouin lasing. As the pump wave is completely coupled with resonances, namely $\Delta\omega_0 = 0$, P_1^c and P_h reach to their maximum values. The minimum threshold of single Brillouin lasing can be derived as $P_{in} = \kappa_1 \kappa_0^2 / (2\kappa_0^c g_1^s)$ when the Brillouin lasing output equals to 0, which is another threshold power description associated with that presented in Ref [9] as $\kappa_1^c \approx \kappa_1$. For the cascaded Brillouin lasing, taking $N = 5$ for an example, $W_4 = k_5/g_5^s$, and the rest W_2 , W_0 can be deduced from W_4 based on Eq. (5). And then W_1 is calculated from the obtained W_0 based on Eq.(4), which is related to $\Delta\omega_0$. Similarly, W_3 and W_5 can be deduced from W_1 based on Eq.(5) as well. Thus, if the last order N^{th} is odd/even number, the even/odd number order lasing is only related to κ_j^i , κ_j^c and g_j^s as that of odd/even number order Brillouin lasing is related to $\Delta\omega_0$. In the following, only single Brillouin lasing is considered.

III. THERMAL PERTURBATIONS ON BRILLOUIN LASING

Two kinds of thermal perturbations on Brillouin lasing are proposed. One is to tune the wavelength λ_p of pump wave, the other is to vary the surrounding temperature. The thermal dynamics of microcavity can be described by [32]:

$$C_m \frac{\partial \Delta T_{ms}(t)}{\partial t} = P_h - P_{out}, \quad (11)$$

where C_m is the thermal capacity of mode area, $\Delta T_{ms}(t)$ is the temperature difference between mode area and surroundings, P_h is the generated thermal power due to material absorption and described by Eq.(10), P_{out} is the dissipated thermal power from mode area to surroundings and calculated by $K \Delta T_{ms}(t)$ when K is defined as the thermal conductivity between mode area and surroundings.

When λ_p is manually tuned by a certain value $\Delta\lambda_p$, the temperature T_m at mode area varies by $\Delta T_m = \Delta\lambda_p / \zeta$ as the resonances are thermally latched by pump wave and ΔT_{ms} is accordingly changed by ΔT_m when the temperature of surroundings T_s keeps unchanged. Thus we know P_{out} varies by $K \Delta T_m$. For a steady state, the left side of Eq. (11) is zero and $P_h = P_{out}$, finally P_h is tuned by $K \Delta T_m$ as well.

For the single Brillouin lasing, in the process of λ_p tuning, other parameters, such as κ_0^i , κ_0^c , κ_1^i , κ_1^c , P_{in} , δ and g_1^s , are all assumed to be not changed when the WGM resonances coupled by pump wave and Brillouin lasing are not altered. Thus only $\Delta\omega_0$ is tuned in order to response to the variation $\Delta P_h = K \Delta T_m$. As shown by Eq. (9) and Eq. (10),

P_1^c and P_h share the same part $X = \sqrt{\frac{2\kappa_0^c P_{in}}{\kappa_1 g_1^s} - \left(\frac{\Delta\omega_0}{g_1^s}\right)^2}$. If X varies by ΔX from $\Delta\omega_0$ tuning, $\Delta P_1^c = 2\kappa_1^c \Delta X$ and $\Delta P_h = 2\delta\kappa_1^i \Delta X$ can be obtained. Therefore, we can get the ratio of the variations of output and thermal powers $\Delta P_1^c / \Delta P_h \approx \kappa_1^c / \delta\kappa_1^i$, and then a relation between $\Delta P_1^c = \Delta P_b$

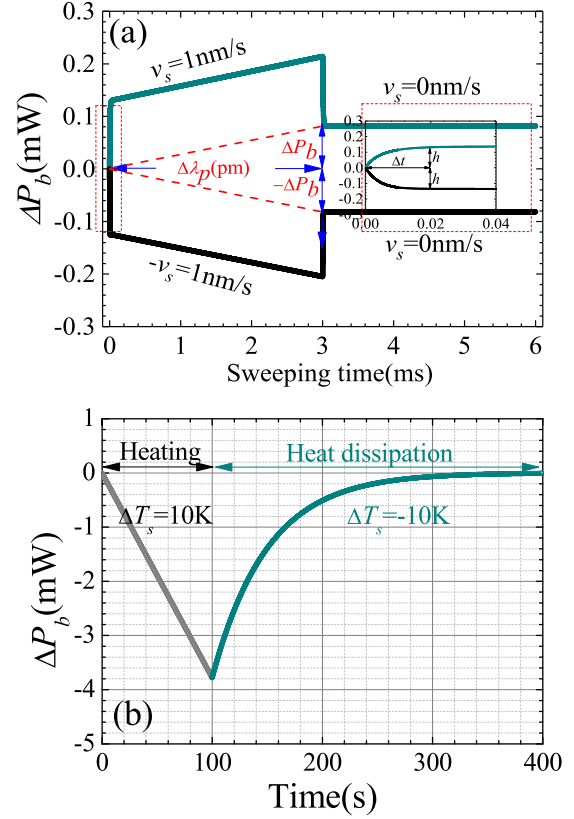


Fig. 2. (a) The variation of the Brillouin microlaser output power ΔP_b as λ_p is swept by 3 pm with a speed of $v_s = \pm 1$ nm/s. The inset is the expanded demonstration of dashed rectangle with the same time scale, where the power coupled into taper $P_{in} = 50$ mW, κ_0^i/κ_0 or $\kappa_1^i/\kappa_1 = 0.2$, $\delta = 0.5$, $g_1^s = 1.75 \times 10^{14}$ Hz²/mW, $C_m = 2.363 \times 10^{-4}$ mJ/K, $K = 4.73 \times 10^{-2}$ mW/K, κ_1 or $\kappa_0 = 2\pi \times 10^6$ Hz and the initial value of $\Delta\omega = \kappa_0$. (b) ΔP_b depending on time for both heating and heat dissipation processes.

and $\Delta\lambda_p$ is approximately bridged:

$$\Delta P_b \approx \frac{\kappa_1^c}{\delta\kappa_1^i} \frac{K}{\zeta} \Delta\lambda_p, \quad (12)$$

as $\Delta P_h = K \Delta\lambda_p / \zeta$, and g_1^s may have a slight change after the tuning of λ_p . Eq. (12) is a theoretical description without considering the resonances transition of both pump wave and Brillouin lasing, and other optical phenomena. If κ_1^c is far greater than κ_1^i and close to κ_1 , most of pump power will be transferred into Brillouin lasing and only a little part of power is transferred into thermal power, which explains that why up to 90% of whole power efficiency can be realized in [9].

Fig.2(a) shows a variation of ΔP_b as λ_p is swept by 3pm with a velocity $v_s = \pm 1$ nm/s from a steady state, which is calculated based on Eq. (11). ΔP_b first jumps by a height of h in a short time of Δt from a thermally steady state to an un-steady state, then linearly increases/decreases following the sweeping of λ_p , and eventually decreases/increases to the secondary steady state with a power jump of h as well. The inset shows the expanded evolution of ΔP_b as λ_p starts sweeping. The jump h is led by the temperature lag of thermal response from λ_p sweeping due to the fact that the temperature can't jump abruptly, where h is proportional to the sweeping speed v_s and Δt is proportional to input power P_{in} . The over

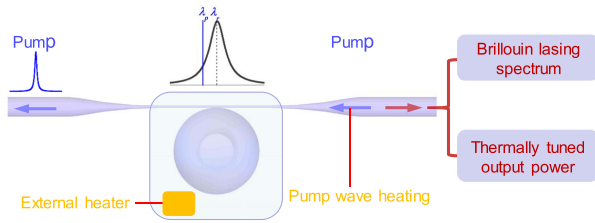


Fig. 3. Schematic illustration of measurement system of Brillouin microsphere laser.

quick sweeping of λ_p generally leads to a great lag of thermal response, if this lag is great enough as the power coupled into cavity is less than the initial value, the resonance does not shift in red direction, but shifts in blue direction and the thermal latching breaks. On the contrary, if λ_p is swept in blue direction, the maximum value of jump power h is equivalent to the initial Brillouin lasing output. Thus, the hopping of lasing output may occur as λ_p is quickly swept.

When we increase/decrease the surrounding temperature T_s by a value of ΔT_s and additionally do not tune λ_p (T_m is unchanged as the resonances are still thermally latched by pump wave), we know ΔT_{ms} decreases/increases by ΔT_s . Similar to that tuning of λ_p , P_{out} or P_h decreases/increases by a value of $K\Delta T_s$ as well for a steady state. In order to response to this thermal change, the detuning $\Delta\omega_0$ is tuned and finally the variation of Brillouin lasing output ΔP_b can be approximately derived from the variation of ΔP_h :

$$\Delta P_b \approx -\frac{\kappa_1^c}{\delta\kappa_1^i} K \Delta T_s. \quad (13)$$

We assume $T_s = T_{s0} + v_h t$ increases linearly as the surroundings is heated, and $T_s = T_{s0} + \Delta T_{s0} e^{-t/\tau}$ decreases exponentially as the heat is dissipated from surroundings, where T_{s0} is the initial temperature, v_h is the temperature increasing speed, and τ is the thermal relax time. In order to mimic the variation in ΔP_b , we set $v_h = 0.1$ K/s, $\tau = 50$ s and the temperature increasing time is 100 s, other parameters are the same as those used in Fig.2(a). The results are shown in Fig. 2(b), the lasing output P_b decreases by a value in 100 s and then recovers to the initial value as the heater cools down for 300 s. P_b follows the change of surrounding temperature T_s and shows no jump. On the other hand, if P_b is tracked by a power meter or oscilloscope, the detection on the evolution of surrounding temperature can be realized.

IV. EXPERIMENTAL DEMONSTRATIONS OF THERMAL PERTURBATIONS ON BRILLOUIN MICROSPHERE LASER

A. Package of Silica Microspheres for Stable Performances of Brillouin Lasing

Fig. 3 shows a schematic illustration of the experiment setup for the measurement of microsphere Brillouin lasers. A tunable external cavity laser (TECL) produced by Photonics Incorporation with the type of Tunics-plus at C band and a typical linewidth of 150 kHz is employed as the pump source, the wavelength resolution of TECL is 1pm, and the typical wavelength and power stability are ± 3 pm/h and ± 0.01 dB/h, respectively. To perform thermal perturbations on the Brillouin

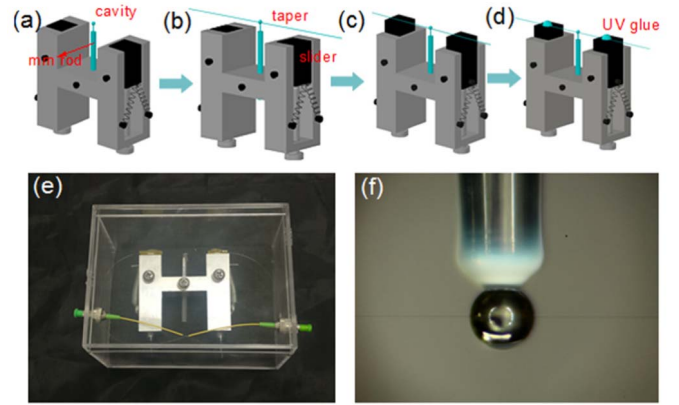


Fig. 4. Packaging steps of the sphere cavity with a fiber taper. (a) A fabricated cavity is firmly fixed by a bolt on a mechanical module; (b) The position of the module with the resonator is tuned by a 3D translation stage to approach to the pulled taper under the monitoring of a microscope. The wide cross section of the sphere cavity allows remarkable coupling tolerance near the equator. (c) The sliders on the module are jacked up to abut against the taper; (d) Ultraviolet(UV) glue is dripped on the top of sliders to fix the taper after several minute solidification. (e) A packaged sphere-taper with two connecting ports. (f) The side view of a sphere cavity coupled with a taper.

laser, sphere cavities fabricated from a 3 millimeter-diameter quartz rod by a mechanical method are employed [13], and a heater, positioned in the box, is used for tuning the temperature of environment. A fiber taper with diameter ranging from $2\mu\text{m}$ to $4\mu\text{m}$, pulled from a single mode fiber, is used to couple the pump wave into the cavity. The power of the backward scattered Brillouin lasing is coupled out by the same taper, then collected by an optical circulator, and subsequently divided into several routes for microlaser diagnosis, for example, using an optical spectrum analyzer (OSA) and a power meter for recording optical spectra and output power. In order to track the real-time variation of the laser output, one of routes is coupled into a photodetector, and the real-time variation of power can be monitored by an oscilloscope.

Before the experimental studies on the thermal characteristics of Brillouin microlasers, a mechanical module is designed and used to package the sphere cavity with a fiber taper in order to stabilize the coupling and achieve stable performances of the Brillouin laser. Detailed packaging steps are presented in Fig. 4(a) to (d). Fig. 4(e) shows a package of the sphere cavity coupled with a fiber taper. Both connectors can be considered as input or output ports for Brillouin lasing. Fig. 4(f) shows the side view of a taper-coupled sphere cavity with a diameter of $\sim 620\mu\text{m}$. The transmission spectrum of the packaged sample is measured and shows typical resonances with Q factors higher than 1×10^8 , which are not spoiled due to the packaging.

In order to couple the pump wave into cavity, the wavelength of the TECL is manually tuned until one of the WGM resonances is thermally latched by the pump wave, the detuning frequency $\Delta\omega_0$ between pump wave and coupled resonance is randomly and passively chosen. If there exists one resonance located in the Brillouin gain curve, the spontaneous Brillouin scattering will be amplified and transformed into SBS due to longer photon life or higher intensity induced by

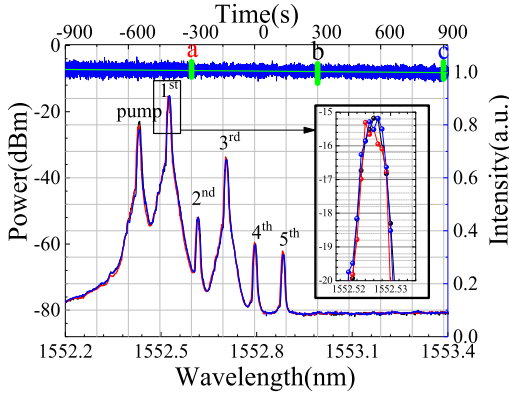


Fig. 5. Three Brillouin lasing spectra recorded in half an hour with time interval of 10 minutes denoted by 'a', 'b' and 'c'. The upper part shows the normalized real time power variation, the slight power decrease (solid line) originates from the slight decrease of pumping power (amplifier). The inset shows the expanded optical spectra of the 1st-order Brillouin lasing peak.

WGM resonances. The detuning Γ between WGM resonance and Brillouin gain curve is also passively chosen and takes effects on intracavity Brillouin gain g_j^s . In order to present the stability of Brillouin microlaser, three optical spectra of a 5-order cascaded Brillouin lasing with a time interval of 10 minutes are measured and shown in Fig. 5. The highest peak is the 1st-order Brillouin lasing while only the backward scattered light is collected. The 1st, 3rd and 5th peaks (from left to right) are the reflected pump wave, the 2nd- and the 4th-order Brillouin lasing, which all result from intra-cavity Rayleigh scattering [34], [35], as the 2nd, 4th and 6th peaks are the 1st-, 3rd- and 5th-order Brillouin lasings. The real time output power is tracked by an oscilloscope and presented in the upper part, the slight decrease of output power is led by the decrease of pump power (amplifier). The inset shows the expanded peak of the 1st-order of Brillouin lasing with a power fluctuation less than 0.2 dBm. The results indicate that the coupling strength between the taper and sphere is stable and the mechanical packaging enables stable performances of Brillouin lasing. By comparing the performances of that un-packaged spheres in free air, where the output is confirmed to be unstable, the results show the coupling noise induced by the displacement of taper and cavity is effectively under control.

B. Wavelength Tuning of Pump Wave

To experimentally investigate thermal behaviors of the Brillouin microsphere laser, the pump wavelength λ_p is firstly swept by steps of 10 pm over the optical resonances until lasing is realized. The tuning step is then minimized to 1 pm. Fig. 6(a) shows a typical variation of lasing output P_b as λ_p is tuned from point 'a' to 'b' and then to 'c' and finally jump to 'd' in a cavity with diameter of $\sim 620 \mu\text{m}$. The pump power P_{in} coupled into the taper is $\sim 100 \text{ mW}$. The total tuning of $\sim 150 \text{ pm}$ can be divided into 7 segments denoted by the number from 1 to 7. In each segment, ΔP_b varies linearly with $\Delta \lambda_p$ with a different slope and a slight deviation. Additionally, the power transitions between adjacent segments are observed. In the following, the detailed explanation on the variation of output power is given.

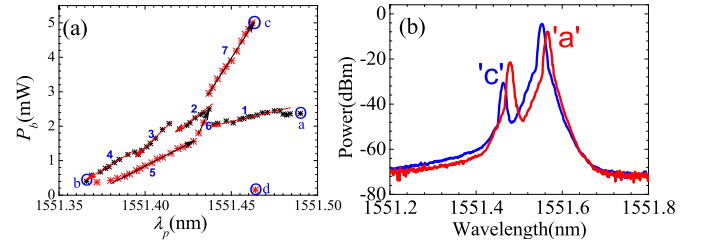


Fig. 6. (a) P_b versus λ_p near $1.55 \mu\text{m}$ as λ_p is firstly tuned from 'a' to 'b' and then tuned back to 'c', and finally to 'd'. (b) The recorded Brillouin lasing spectrum near point 'c' and point 'a'.

Firstly, as the pump is tuned in blue direction from point 'a' (segment 1), the coupled resonance λ_r of pump wave, following the shift of λ_p , drifts to shorter wavelength and the thermal power P_h decreases. As described by Eq. (9) to Eq. (12), $\Delta P_b / \Delta \lambda_p$ is related to the system parameters κ_0^i , κ_0^c , κ_1^i , κ_1^c , P_{in} , δ , g_1^s and $\Delta \omega_0$. If both the resonances coupled by pump wave and Brillouin lasing are not skipped, κ_0^i , κ_0^c , κ_1^i , κ_1^c and δ can be assumed to not change and only $\Delta \omega_0$ changes to response to the thermal variation in mode (g_1^s may have a slight change during λ_p sweeping). As predicted by Eq. (12), the linear dependences of ΔP_b on $\Delta \lambda_p$ are observed. However, as λ_p is further tuned, at the end of segment 1 and the beginning of segment 2, the lasing output transition happens, it means the coupled resonance of pump wave or Brillouin lasing is skipped from one resonance to another and the slope $\Delta P_b / \Delta \lambda_p$ is accordingly changed. The output transition cannot be attributed to the resonance transition of pump wave, it is because only when $P_h(P_c)$ decreases to zero, the coupled resonance can't follow the tuning of λ_p and the resonance transition happens. Thus, we attribute this power transition to the mode skip of lasing between different resonances, since that the Brillouin gain bandwidth (a few tens of megahertz) may cover several resonances of large sphere cavities (this can be confirmed from the measured transmission spectrum) and the lasing competition between resonances may exist. As λ_p is tuned continuously in blue direction, similar performances are observed in segments 2 to 4.

Secondly, as the pump is tuned in red direction from point 'b', more and more power is coupled into cavity and all the WGM resonances drift synchronously due to thermal effects (segments 5 to 7). If the pump power coupled into cavity P_c increases to the maximum value for the coupled resonance, namely $\lambda_p - \lambda_r \approx 0$ or $\Delta \omega_0 \approx 0$, the thermal power P_h also reach its maximum value and can't support the resonance shift as the pump λ_p is further tuned, the resonance latching breaks and P_c decreases to zero. The resonances start to shift in blue direction during the process of heat dissipation until another twins resonances are involved in the coupling of pump wave and Brillouin lasing. Thus, power transitions between 5 and 6, 6 and 7 maybe led by the resonances transition of only Brillouin lasing or both pump wave and Brillouin lasing. At last, if there is no resonances to match both pump wave and Brillouin lasing, P_c or P_b decreases to 0 (point 'd').

Finally, in Fig. 6(b), the Brillouin lasing spectra near point 'c' and point 'a' are presented. As observed in the

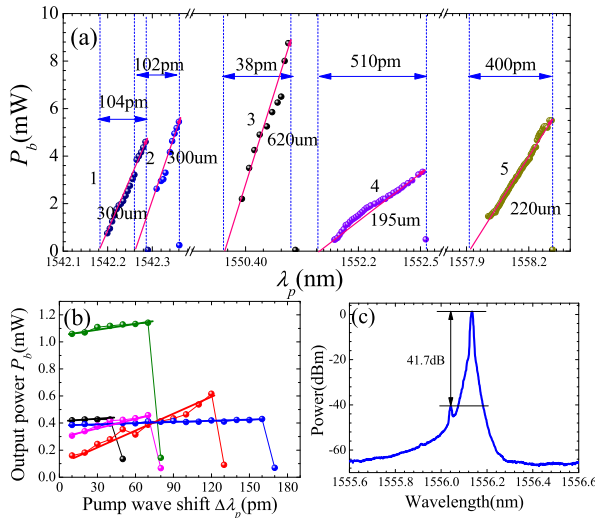


Fig. 7. (a) P_b versus λ_p in samples with diameters ranging from $\sim 200\mu\text{m}$ to $\sim 600\mu\text{m}$. (b) several results of P_b depending on the shift of pump wave $\Delta\lambda_p$ in a sample with diameter of $\sim 300\mu\text{m}$ under pump power $P_{in} \approx 72\text{mW}$. (c) A Brillouin lasing spectrum with SMSR of 41.7 dB.

measurements, the amplitude of backward pump wave led by Rayleigh scattering is usually lower as that of Brillouin lasing is higher. In other words, the Brillouin lasing extracts more power from the coupled pump wave in cavity and the left for Rayleigh scattering is accordingly lower. The optical bistabilities due to the resonance transition of pump wave and Brillouin lasing are quite universally observed in large cavities with intense resonances.

In the following, we give five typical results from four samples with diameters ranged from $\sim 200\mu\text{m}$ to $\sim 600\mu\text{m}$, including two results from a $\sim 300\mu\text{m}$ -diameter cavity. As shown in Fig. 7 (a), where we estimate the total tuning bandwidth Λ_w by extrapolating the lasing output P_b to zero, since we cannot fully tune the pump λ_p as the thermal latching state will be broken when λ_p is continuously tuned in red direction. Λ_w is 104 pm and 102 pm for the 300 μm -diameter cavity, and 38 pm, 510 pm and 400 pm for cavities with diameters of $\sim 620\mu\text{m}$, $\sim 195\mu\text{m}$ and $\sim 220\mu\text{m}$, respectively. As shown by Eq.(10), Λ_w is determined by the maximum thermal power as $\Delta\omega_0 = 0$ and related to P_{in} , κ_0^c , κ_1^i , κ_1^s , g_1^s and δ . Thus, it is difficult to obtain the definite value of Λ_w when some parameters are not known. Moreover, the results show that the cavity with larger dimension usually has a greater $\Delta P_b/\Delta\lambda_p$, which is consistent with theoretical prediction in Eq.(12) since that a larger cavity with greater thermal dissipation area usually has a greater K . Fig.7(b) presents several results of P_b depending on the shift of pump wave $\Delta\lambda_p$ (tuning step is 10pm). The measurements are performed in a microsphere of diameter $\sim 300\mu\text{m}$ with a pump power $P_{in} \approx 72\text{mW}$. The results show that the changing rate $\Delta P_b/\Delta\lambda_p$ varies from different measurements, or the different twins resonances coupled by pump wave and Brillouin lasing, even under the same P_{in} . In Fig. 7(c), we give a measured spectrum from a $\sim 300\mu\text{m}$ -diameter Brillouin laser, where the lasing output is $\sim 26.2\text{mW}$ and the total power conversion efficiency is estimated to be 67%~87%. The demonstrated

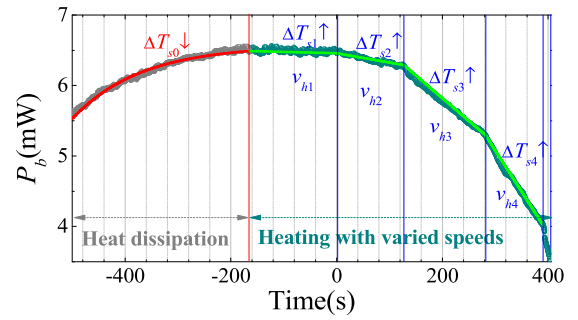


Fig. 8. Brillouin lasing output versus thermal tuning time. Both heat dissipation and heating processes are considered.

41.7 dB of SMSR, to the best of our knowledge, is the highest reported value to date in WGM Brillouin microlasers.

C. Temperature Variations of Surroundings

The thermal influences on Brillouin microlaser induced by temperature variations of surroundings are also studied. Firstly, the system is heated up to a certain temperature $T_s = T_{s0} + \Delta T$ (T_{s0} is the room temperature). And then heating stops, the lasing output is recorded within a few minutes as the thermal power is dissipated from the heater into the rest part of space, T_s productively decreases. Finally, the electric heater is operated again with different applied voltages or heating-up speeds and time. In both T_s decreasing and increasing processes, the wavelength of pump wave is not tuned, which means that the resonances have no shift or the temperature at mode area is not changed. As shown in Fig. 8, the measured lasing output depending on the time are fitted well by assuming that T_s decreases exponentially as the thermal power is dissipated from the heater and increases linearly with different speeds (v_{h1} to v_{h4}) as the heater is heated up under driven of different voltages. ΔT_{s0} , ΔT_{s1} , ΔT_{s2} , ΔT_{s3} , ΔT_{s4} are the temperature variations and the arrows denote the temperature increasing or decreasing. Here, we do not give the estimated ΔT_{s0} , ΔT_{s1} , ΔT_{s2} , ΔT_{s3} , ΔT_{s4} since that the parameters of the photonic system, such as K , δ and g_1^s are all unknown. The lasing output power, as predicted by Eq.(13), varies linearly with surroundings temperature T_s . In addition, the higher the heating speed ($v_{h1} < v_{h2} < v_{h3} < v_{h4}$), the faster the Brillouin lasing output decreases, this further confirms that the Brillouin lasing output heavily depends on surrounding temperature. The results indicate that the Brillouin lasing holds potential for the application of thermal sensing.

V. CONCLUSION

In conclusion, the thermal characteristics of Brillouin silica microsphere lasers have been investigated. The constructed analytic model based on coupled mode theory predicts that the output power of Brillouin lasing varies linearly with the resonant shift induced by the thermal perturbations. In order to verify this prediction, mechanically packaged silica microspheres are employed and experiments are simply performed by either tuning the wavelength of pump wave or varying the environmental temperature. The results confirm our theoretical prediction. Some optical phenomena, such as optical bistabilities induced by the resonant transition of pump wave and

Brillouin lasing, and lasing spectrum of up to ~ 41.7 dB SMSR are demonstrated. By simply tracking the output power of Brillouin laser with a power meter, we can know the temperature evolution of environments resulting in the shift of microsphere resonances. Except thermal perturbation, optical perturbations on evanescent wave, such as adherence of biomolecules and optical coupling from a probe light, may also be detected from the variation of Brillouin lasing output power. Being different from the detecting on the shift of resonances which is usually performed under low pump power to eliminate thermal effect and can realize detecting accuracy of nano-K [36], the current detecting accuracy ($1\sim 2$ pm or $(1\sim 2)/13.89$ K) here is limited by the thermal noises induced by the strong interaction between material and high density photon at coupling place and in the microsphere. We wish our preliminary work can promote the application of microlasers and the detecting accuracy can be further improved in the future.

REFERENCES

- [1] R. Y. Chiao, C. H. Townes, and B. P. Stoicheff, "Stimulated Brillouin scattering and coherent generation of intense hypersonic waves," *Phys. Rev. Lett.*, vol. 12, no. 21, pp. 592–595, 1964.
- [2] E. P. Ippen and R. H. Stolen, "Stimulated Brillouin scattering in optical fibers," *Appl. Phys. Lett.*, vol. 21, no. 11, pp. 539–541, 1972.
- [3] A. Kobayakov, M. Sauer, and D. Chowdhury, "Stimulated Brillouin scattering in optical fibers," *Adv. Opt. Photon.*, vol. 2, no. 1, pp. 1–59, 2010.
- [4] E. Garmire, "Perspectives on stimulated Brillouin scattering," *New J. Phys.*, vol. 19, p. 011003, Jan. 2017.
- [5] R. Pant *et al.*, "On-chip stimulated Brillouin scattering," *Opt. Exp.*, vol. 19, no. 9, pp. 8285–8290, Apr. 2011.
- [6] B. Morrison *et al.*, "Compact Brillouin devices through hybrid integration on silicon," *Optica*, vol. 4, no. 8, pp. 847–854, 2017.
- [7] H. Shin *et al.*, "Tailorable stimulated Brillouin scattering in nanoscale silicon waveguides," *Nature Commun.*, vol. 4, pp. 1–10, 2013, Art. no. 1944.
- [8] J.-Z. Zhang and R. K. Chang, "Generation and suppression of stimulated Brillouin scattering in single liquid droplets," *J. Opt. Soc. Amer. B, Opt. Phys.*, vol. 6, no. 2, pp. 151–153, 1988.
- [9] I. S. Grudin, A. B. Matsko, and L. Maleki, "Brillouin lasing with a CaF₂ whispering gallery mode resonator," *Phys. Rev. Lett.*, vol. 102, no. 4, p. 043902, 2009.
- [10] M. Tomes and T. Carmon, "Photonic micro-electromechanical systems vibrating at X-band (11-GHz) rates," *Phys. Rev. Lett.*, vol. 102, no. 11, p. 113601, 2009.
- [11] G. Bahl, J. Zehnpfennig, M. Tomes, and T. Carmon, "Stimulated optomechanical excitation of surface acoustic waves in a microdevice," *Nature Commun.*, vol. 2, no. 1, p. 403, 2011.
- [12] C. Guo *et al.*, "Ultralow-threshold cascaded Brillouin microlaser for tunable microwave generation," *Opt. Lett.*, vol. 40, no. 21, pp. 4971–4974, 2015.
- [13] K. Che *et al.*, "Ultra-high Q sphere-like cavities for cascaded stimulated Brillouin lasing," *Opt. Commun.*, vol. 387, pp. 421–425, Mar. 2017.
- [14] C. L. Guo *et al.*, "Low-threshold stimulated Brillouin scattering in high-Q whispering gallery mode tellurite microspheres," *Opt. Exp.*, vol. 23, no. 25, pp. 32261–32266, 2015.
- [15] P. Del, "Haye, S. A. Diddams, and S. B. Papp, "Laser-machined ultra-high-Q microrod resonators for nonlinear optics," *Appl. Phys. Lett.*, vol. 102, no. 22, p. 221119, 2013.
- [16] M. Asano *et al.*, "Stimulated Brillouin scattering and Brillouin-coupled four-wave-mixing in a silica microbottle resonator," *Opt. Exp.*, vol. 24, no. 11, pp. 12082–12092, 2016.
- [17] Q. J. Lu, S. Liu, X. Wu, L. Y. Liu, and L. Xu, "Stimulated Brillouin laser and frequency comb generation in high-Q microbubble resonators," *Opt. Lett.*, vol. 41, no. 8, pp. 1736–1739, 2016.
- [18] A. A. Savchenkov, A. B. Matsko, V. S. Ilchenko, D. Seidel, and L. Maleki, "Surface acoustic wave opto-mechanical oscillator and frequency comb generator," *Opt. Lett.*, vol. 36, no. 17, pp. 3338–3340, 2011.
- [19] G. Lin *et al.*, "Cascaded Brillouin lasing in monolithic barium fluoride whispering gallery mode resonators," *Appl. Phys. Lett.*, vol. 105, no. 23, p. 231103, 2014.
- [20] H. Lee *et al.*, "Chemically etched ultrahigh-Q wedge-resonator on a silicon chip," *Nature Photon.*, vol. 6, pp. 369–373, May 2012.
- [21] J. Li, H. Lee, and K. J. Vahala, "Microwave synthesizer using an on-chip Brillouin oscillator," *Nature Commun.*, vol. 4, no. 12, p. 2097, Jun. 2013.
- [22] A. Choudhary *et al.*, "Tailoring of the Brillouin gain for on-chip widely tunable and reconfigurable broadband microwave photonic filters," *Opt. Lett.*, vol. 41, no. 3, pp. 436–439, Feb. 2016.
- [23] C.-H. Dong, Z. Shen, C.-L. Zou, Y.-L. Zhang, W. Fu, and G.-C. Guo, "Brillouin-scattering-induced transparency and non-reciprocal light storage," *Nat. Commun.*, vol. 6, p. 6193, Feb. 2015.
- [24] J.-H. Kim, M. C. Kuzyk, K. Han, H. Wang, and G. Bahl, "Non-reciprocal Brillouin scattering induced transparency," *Nature Phys.*, vol. 11, no. 3, pp. 275–280, 2015.
- [25] J. Li, M.-G. Suh, and K. Vahala, "Microresonator Brillouin gyroscope," *Optica*, vol. 4, no. 3, pp. 346–348, 2017.
- [26] A. Chiasera *et al.*, "Spherical whispering-gallery-mode microresonators," *Laser Photon. Rev.*, vol. 4, no. 3, pp. 457–482, 2010.
- [27] B. E. Little, S. T. Chu, H. A. Haus, J. Foresi, and J.-P. Laine, "Microring resonator channel dropping filters," *J. Lightw. Technol.*, vol. 15, no. 6, pp. 998–1005, 1997.
- [28] B. Min, T. J. Kippenberg, and K. J. Vahala, "Compact, fiber-compatible, cascaded Raman laser," *Opt. Lett.*, vol. 28, no. 17, pp. 1507–1509, 2003.
- [29] M. L. Gorodetsky and V. S. Ilchenko, "Optical microsphere resonators: Optimal coupling to high-Q whispering-gallery modes," *J. Opt. Soc. Amer. B*, vol. 16, no. 1, pp. 147–154, 1999.
- [30] L. Mescia, P. Bia, M. De Sario, A. Di Tommaso, and F. Prudenzano, "Design of mid-infrared amplifiers based on fiber taper coupling to erbium-doped microspherical resonator," *Opt. Exp.*, vol. 20, no. 7, pp. 7616–7629, Mar. 2012.
- [31] Y. Dumeige, S. Trebaol, L. Ghiša, T. K. N. Nguyễn, H. Tavernier, and P. Féron, "Determination of coupling regime of high-Q resonators and optical gain of highly selective amplifiers," *J. Opt. Soc. Amer. B, Opt. Phys.*, vol. 25, no. 12, pp. 2073–2080, 2008.
- [32] T. Carmon, L. Yang, and K. J. Vahala, "Dynamical thermal behavior and thermal self-stability of microcavities," *Opt. Exp.*, vol. 12, no. 20, pp. 4742–4750, 2004.
- [33] Q. Ma, T. Rossmann, and Z. Guo, "Temperature sensitivity of silica micro-resonators," *J. Phys. D, Appl. Phys.*, vol. 41, no. 24, p. 245111, 2008.
- [34] M. L. Gorodetsky, A. D. Pryamikov, and V. S. Ilchenko, "Rayleigh scattering in high-Q microspheres," *J. Opt. Soc. Amer. B*, vol. 17, no. 6, pp. 1051–1057, 2000.
- [35] T. J. Kippenberg, S. M. Spillane, and K. J. Vahala, "Modal coupling in traveling-wave resonators," *Opt. Lett.*, vol. 27, no. 19, pp. 1669–1671, 2002.
- [36] D. V. Strelakov, R. J. Thompson, L. M. Baumgartel, I. S. Grudin, and N. Yu, "Temperature measurement and stabilization in a birefringent whispering gallery mode resonator," *Opt. Exp.*, vol. 19, no. 15, pp. 14495–14501, 2011.

Kaijun Che was born in Linchuan, Jiangxi, China, in 1985. He received the Ph.D. degree in physical electronics from the Institute of Semiconductor, Chinese Academy of Science, in 2010. He is currently an Associate Professor with the Department of Electronics Engineering, Xiamen University, Xiamen, Fujian, China, and visiting the Department of Electronic and Electrical Engineering, The University of Sheffield, U.K. His research interests include semiconductor microlasers, plasmonic microdevices, optical nonlinearities, and optical devices' applications.

Deyu Tang was born in Xinyang, Henan, China. He received the B.Sc. degree in microelectronics from Xiamen University, Xiamen, Fujian, in 2015, where he is currently pursuing the master's degree with the Department of Electronics Engineering.

Changyan Ren was born in Shiyan, Hubei, China, in 1991. She received the B.Sc. degree in microelectronics from the Wuhan University of Technology, Wuhan, Hubei, in 2015. She is currently pursuing the master's degree with the Department of Electronics Engineering, Xiamen University, Xiamen, Fujian, China.

Huiying Xu was born in Fujian, China, in 1963. She received the B.S. degree in physics from the Physics Department, Xiamen University, Xiamen, China, in 1985, and the D.E.A. degree from the University of Rennes I, France, in 2001. She is currently a Full Professor with the Department of Electronics Engineering, Xiamen University. Her research interests involve optical telecommunication, laser technology and its applications, and optical fiber devices.

Lujian Chen was born in Xiamen, Fujian, China, in 1980. He received the Ph.D. degree from the Material School, Zhejiang University, in 2007. He is currently an Associate Professor with the Department of Electronics Engineering, Xiamen University, Xiamen, Fujian. His research focuses on DFB lasers, cholesteric liquid crystals, and WGM microlasers.

Chaoyuan Jin was born in Hangzhou, Zhejiang, in 1978. He received the Ph.D. degree in electronic and electrical engineering from The University of Sheffield, U.K., in 2008. He was awarded a JSPS Post-Doctoral Fellowship and involved in quantum dot switches at Kobe University, Japan, from 2008 to 2010. In 2010, he joined the Eindhoven University of Technology, The Netherlands, as a Post-Doctoral Researcher, where he was involved in the ultrafast control of cavity quantum electrodynamics based on single quantum dots coupled to photonic crystal cavities. From 2013 to 2015, he moved into industry with EFFECT Photonics B.V. In his role as a Senior Photonics Scientist, he developed high-speed optical transceivers for short-reach optical communications based on generic photonic integration technologies. He is currently a Vice-Chancellor's Fellow, developing research programs on ultrafast photonic devices at the Department of Electronic and Electrical Engineering, The University of Sheffield. His research activities have been focused on nano-photonic devices for optical signal and quantum information processing, including optical switches, lasers, single-photon sources, and nano-photonic integrated circuits.

Zhiping Cai was born in Fujian, China, in 1965. He received the Ph.D. degree from the University of Nice, Nice, France, in 1989. He was a Senior Visiting Scholar from 1994 to 1996 and a Guest Professor from 2000 to 2001 with ENSSAT, Lannion, France. He also visited the University of Cambridge for one month in 2013, and the École Normale Supérieure for three months in 2012. Since 1998, he has been a Full Professor with the Department of Electronics Engineering, Xiamen University, Xiamen, China. He has authored over 100 publications in refereed journals and conference proceedings. His research interests cover laser physics, optoelectronics, meso-optics, and their applications.